Available online at www.sciencedirect.com
SCIENCE DIRECT®
Earth and Planetary Science Letters 227 (2004) 481–490
EPSL
www.elsevier.com/locate/epsl

Growth rates of the deep-sea scleractinia *Desmophyllum cristagalli* and *Enallopsammia rostrata*

J.F. Adkins[a,*], G.M. Henderson[b], S.-L. Wang[a], S. O'Shea[c], F. Mokadem[b]

[a]*Deptartment of Geology and Planetary Sciences, MS 100-23, Caltech, Pasadena, CA 91125, United States*
[b]*Department of Earth Sciences, Parks Road, Oxford OX1 3PR, UK*
[c]*NIWA, 310 Evans Bay Parade, Greta Point, PO Box 14-901, Kilbirnie, Wellington, New Zealand*

Received 15 March 2004; received in revised form 6 August 2004; accepted 30 August 2004
Editor: E. Bard

Abstract

With uranium rich skeletons and density bands similar to their surface coral counterparts, deep-sea scleractinia are a promising archive of past climate. To improve the utility of fossil samples as monitors of deep ocean variability, we have measured ^{210}Pb and ^{226}Ra activities in a variety of modern specimens to constrain the range of growth rates. Mechanical and chemical cleaning of each sample are required to isolate the radionuclides trapped in the coral skeleton from surface contaminants. However, in many cases mechanically cleaned samples show the same overall growth rate as parallel transects of samples subjected to the full chemical and mechanical cleaning but with much higher overall activities. Three samples of *Desmophyllum cristagalli* show a range of vertical extension rates from 0.5 mm/yr to 2 mm/yr, consistent with previous estimates. A single *Enallopsammia rostrata* from the North Atlantic is over 100 years old. Its average radial growth rate is 0.07 mm/yr, and the clear banding in this direction is not consistent with annual periodicity. A minimum vertical extension rate of 5 mm/yr is estimated from the ^{210}Pb data. Both of these species are found in the fossil record and, with the growth rates determined here, can record about 100 years of climate change. The growth rates will allow the reconstruction of climate at subdecadal resolution in *D. cristagalli* and even higher resolution in *E. rostrata*.

1. Introduction

Reef building surface corals are an important archive of ocean temperature and salinity variability at subannual resolution over many different time periods [1–4]. Their usefulness arises from two key factors: they contain climate-related geochemical tracers in their skeleton and they have annual growth bands [5]. Surface coral annual banding and growth rates were first established using the nuclear bomb-produced radionuclides around Eniwetok Atoll [6]. Bands of radioactive material (chiefly ^{90}Sr) were imaged in slabs of coral with photographic paper, and the number of density band pairs between these hot

* Corresponding author.
E-mail address: jess@gps.caltech.edu (J.F. Adkins).

0012-821X/$ - see front matter © 2004 Elsevier B.V. All rights reserved.
doi:10.1016/j.epsl.2004.08.022

spots corresponded to the number of years between nuclear tests. This was a conclusive demonstration that the banding in surface corals is annual.

This elegant use of marine radionuclides was soon augmented with studies using naturally produced decay products [7–9]. These studies used the ^{226}Ra–^{210}Pb parent–daughter pair and ^{228}Ra activities, assuming closed system first order decay, to calculate growth rates. The governing first order differential equation in this case is:

$$^{210}\mathrm{Pb}_{\mathrm{ex}} = {}^{210}\mathrm{Pb}^{0}_{\mathrm{ex}} e^{-\lambda z/r} \quad (1)$$

where ^{210}Pb$_{ex}$ is the measured activity of ^{210}Pb above that supported by decay of ^{226}Ra, ^{210}Pb$^{0}_{ex}$ is the initial excess at the time of incorporation, r is the growth rate, z is the distance from the growing surface, and λ is the ^{210}Pb decay constant (0.03067 yr^{-1}). With this equation, measured profiles of ^{210}Pb and ^{226}Ra in biogenic carbonates can constrain the mean extension rate, provided that there have not been significant changes in ^{210}Pb$^{0}_{ex}$ with time. All lines of evidence in surface corals—bomb nuclides, naturally produced nuclides, seasonally varying tracers, and growth band thickness—show growth rates of around 1 cm/yr in the mean but with wide variance between samples and locations.

Recently, deep-sea corals have been exploited as archives of oceanic variability [10–12]. However, studies of the geochemistry and age structure of this new archive are still at an early stage. For deep-sea corals to become reliable recorders of past ocean variability at high resolution, the nature of their banding and their growth rates needs to be better characterized. Early observations of the scleractinian deep-sea coral *Lophelia pertusa* growing on submerged trans-Atlantic cables gave minimum growth rates of 4–8 [13] and ~6 mm/yr [14]. More recently, this species was found on North Sea oil rigs and found to have a minimum extension rate of 26 mm/yr [15]. An early radiometric dating study of the gorgonian *Corallium niobe*, using ^{210}Pb, found a radial growth rate of 0.11 mm/yr [16]. More recent work on gorgonians using ^{14}C have estimated that *Primnoa resedaeformis* has a radial growth rate of 0.044 mm/yr and a tip extension rate of 1.5–2.5 mm/yr [17]. A single Holocene age *Desmophyllum cristagalli* had a bottom minus top ^{14}C age of 70±28 years, which implied a vertical extension rate of ~0.7 mm/yr [18], in agreement with U/Th data from this same species [19].

In summary, previous estimates of deep-sea coral growth rates, from mostly nonscleractinian species, range over a factor of 200. It is therefore important to better understand the growth rates of the more commonly utilized species for paleoclimate studies so that their potential as archives of seasonal, interannual, and decadal environmental change can be assessed. In this paper, we attempt a systematic study of the growth rates of two scleractinia deep-sea corals which show promise for paleoclimate studies. Using the ^{226}Ra–^{210}Pb technique, we evaluate cleaning methods and measure age profiles in three modern *D. cristagalli* from the South Pacific (samples I685, S130, and G200) and a single modern *Enallopsammia rostrata* from the North Atlantic (sample ALV 3701-8). Our results provide the most accurate available assessment of growth rate for the former and the first assessment for the latter.

2. Methods

Whole coral samples were mechanically cleaned of exterior contamination with a Dremel tool and a diamond abrasion wheel. Noncoral carbonate cleaned from the surface included encrusting sponges and worm tubes. Sediment trapped inside the coral and between the septa was removed with deionized water and a toothbrush. Once corals were sectioned into ~1.5-g samples, more sediment was removed by further scrubbing. All samples underwent this preliminary mechanical cleaning, but some subsamples were further cleaned, following the chemical precleaning procedure of Adkins and Boyle [20]. This H_2O_2/NaOH and H_2O_2/$HClO_4$ procedure removes adsorbed radionuclides from the coral's exterior and dissolves ~10% of the mass of each sample. Samples cleaned with the full procedure are hereafter referred to as "chemically cleaned", while those not subjected to this full treatment are referred to as "mechanically cleaned".

^{210}Pb activity in each sample was determined by alpha counting of ^{210}Po, assuming secular equilibrium between ^{210}Pb and ^{210}Po within the coral lattice. Samples were dissolved in 15 ml of 2N HCl and spiked with ~0.5 g of a 1.8-dpm/g ^{209}Po solution. This

solution was heated to dryness and then oxidized in 2 ml of 2% $HClO_4$ to remove organics that can bind Po. The residue was redissolved in 2N HCl and transferred to a new 125-ml beaker. Plating of Po onto silver disks followed the procedure of Flynn [21]. Due to the presence of Fe^{III} in our oxidized samples, we included a 20% hydroxylamine solution in the plating reagents. This reductant prevented Fe oxides from coating the Ag disk and thereby limiting the Po activity. Plating was kept to a single face of the silver disk by using modified magnetic stirrers to hold the silver in a constant orientation. Disks were counted for their ^{209}Po and ^{210}Po activities at the Lamont–Doherty Earth Observatory. The use of hydroxylamine and modified magnetic stirrers ensured high chemical yields of Po between 70% and 90%. Uncertainties for the ^{210}Pb analyses were assessed from counting statistics of the measured alpha decays.

An accurately weighed aliquot equivalent to approximately 0.25 g of coral material was taken from the plating solution of each sample. This aliquot was analyzed for ^{226}Ra concentrations using isotope-dilution atom counting techniques, as described in Foster et al. [22]. Briefly, spikes of ^{228}Ra and ^{229}Th were added (the latter is used to assess the removal of ingrown ^{228}Th from the spike during chemical separation). After fully drying the sample to ensure spike equilibration, the Ra is separated from the carbonate matrix by a four-column ion-exchange process. ^{228}Ra/^{226}Ra ratios were measured on resulting Ra separates using a Nu Instruments Inductively Coupled Plasma Mass Spectrometer (ICP-MS) equipped with multiple ion counters. This technique yields ^{226}Ra concentrations with an uncertainty of approximately 2%, including counting errors, blank and gain error, and weighing error. The accuracy of the technique has been confirmed by previous measurement of seawater samples with known concentrations.

3. Results

Activities of ^{210}Pb in blanks run throughout the period of sample processing were always within error of the detector backgrounds (n=7). A single ^{226}Ra blank on the entire procedure was also low at 0.012 dpm, equivalent to 3% of the average analyzed sample. Most of this blank was introduced during the plating procedure, and blanks during chemical separation of the Ra were negligible. All sample ^{226}Ra concentrations have been corrected for the full procedural blank. Sample replicates are shown in Table 1. These were measured by dissolving a sample 2 or 3 times larger than normal, splitting the solution into equal portions, spiking the individual splits, and then plating the samples as normal. All replicates with significant activity agree within the counting statistics errors. At its base, coral 36544 has very low activity (replicates M, N, and P), and one of the three samples does not fall within the analytical uncertainty.

Profiles of ^{210}Pb and ^{226}Ra activity in a mechanically cleaned *D. cristagalli* sample from south of New Zealand (G200; 43°54.0′S, 179°44′W, 395 m) are shown in Fig. 1. The ^{226}Ra parent shows a constant profile of just under 0.4 dpm/g in both parallel transects. This implies an effective distribution coefficient (D_{Ra}=(^{226}Ra/Ca)$_{coral}$/(^{226}Ra/Ca)$_{seawater}$) for ^{226}Ra into coral aragonite of ~4 (given a ^{226}Ra concentration at ~400 m in nearby GEOSECS Station #296 of ~10 dpm/100 kg). This number is similar to the range of values (D_{Ra}=1.3–2.7) we calculate for a deep-sea coral from the Atlantic analyzed by Druffel et al. [16]. Calculation of distribution coefficients in this way does not imply an assessment of the true thermodynamic equilibrium coefficient (K) for partitioning between solid calcium carbonate and seawater. Instead, the distribution coefficient (D) is an empirical value based on local seawater and measured values for the coral lattice. It represents the combined effects of

Table 1
Replicate analyses of ^{210}Pb and ^{226}Ra activity in the deep-sea coral *D. cristagalli* to demonstrate data quality

Sample #	[210] (dpm/g)	1σ error (dpm/g)	[^{226}Ra] (dpm/g)	1σ error (dpm/g)
36544-C	0.095	0.007		
36544-D	0.090	0.005		
36544-M	0.065	0.002		
36544-N	0.020	0.001		
36544-P	0.058	0.003		
G200P-M	0.287	0.005		
G200P-N	0.282	0.005	0.237	0.002
G200P-P	0.268	0.005	0.245	0.003
I685P-1	0.294	0.005		
I685P-2	0.298	0.005		

Most ^{210}Pb data agree at the 2σ level. For one triplicate with very low activity, this was not true. The single ^{226}Ra replicate shows good agreement.

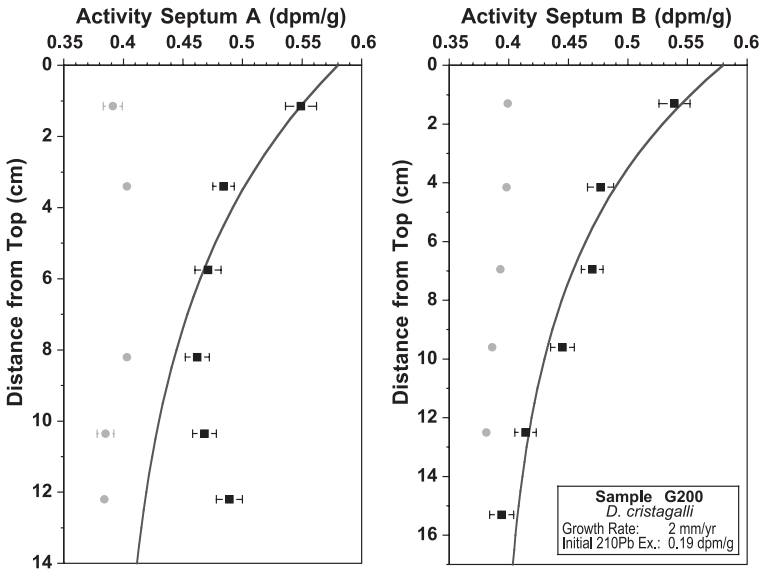

Fig. 1. ^{210}Pb (black squares) and ^{226}Ra (gray circles) data from *D. cristagalli* sample G200. Radionuclide activity error bars on this and all subsequent figures are the 1σ counting statistics estimates. The gray line in both panels is the solution to Eq. (1), with a growth rate of 2 mm/yr and a $^{210}Pb_{ex}^{0}$ of 0.19 dpm/g.

thermodynamics and the complexities of biomineralization of the coral aragonite.

^{210}Pb activity is clearly in excess of the ^{226}Ra activity in all subsamples of G200 except at the base of septum B. Two processes determine the shapes of both Pb profiles. First, initial ^{210}Pb excess is incorporated into the coral skeleton during growth and decays back to the ^{226}Ra parent, with time following Eq. (1). Second, relatively insoluble ^{210}Pb can be added from seawater anywhere along the exterior of the skeleton and at any time after the initial aragonite growth. The most straightforward explanation of the data is that the trend towards lower activity further from the coral's top in both sample transects represents the first closed-system process, while the increase at the base of transect A shows the second open-system source of ^{210}Pb.

These two processes are also apparent in a second mechanically cleaned *D. cristagalli* sample (S130; 43°34.0′S, 175°57′E, 335 m) shown in Fig. 2. Here, open-system addition of ^{210}Pb is apparent in the middle of the coral, while the initial $^{210}Pb_{ex}$ has decayed back to near secular equilibrium throughout the rest of the profile. Three samples from this coral's pedicil show lower ^{210}Pb activity than the main skeleton, indicating either an earlier formation time or a different distribution coefficient for this original and distinct $CaCO_3$ material.

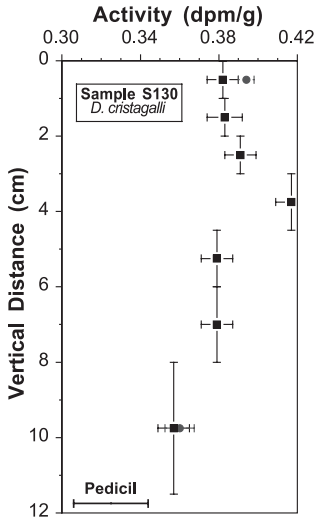

Fig. 2. ^{210}Pb (black squares) and ^{226}Ra (gray circles) data from *D. cristagalli* sample S130. The black line near the bottom is the range of three ^{210}Pb measurements of the corals pedicil. Except for one sample at 4 cm, all of the data are within error of a constant ^{210}Pb profile of 0.38 dpm/g. This result implies that the coral was dead for longer than ~100 years before it was sampled from the sea floor.

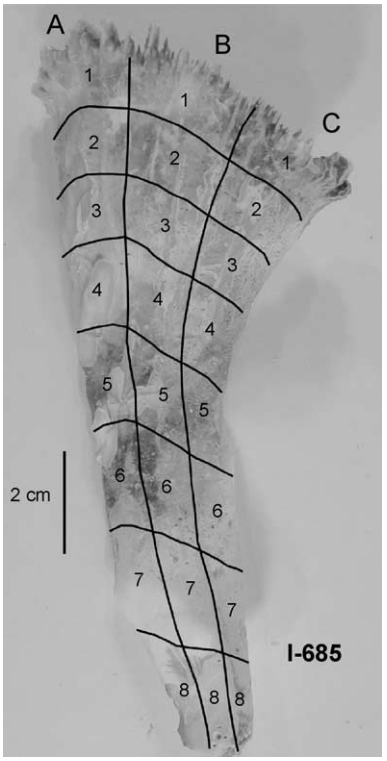

Fig. 3. Photograph of *D. cristagalli* sample I685. Black lines show where individual subsamples were cut with a Dremel tool to form the three parallel transects.

Using the mechanical and chemical cleaning procedure described above, we can separate the open- and closed-system processes within a single *D. cristagalli*. Three parallel vertical sampling transects of a third *D. cristagalli* sample (I685, 48°19.5′S, 179°29.5′W, 722 m) are shown in Fig. 3. Two of these were fully chemically cleaned, as described above (A and B), and the third (C) was only mechanically cleaned. The resulting ^{210}Pb and ^{226}Ra profiles are shown in Fig. 4. Chemical cleaning clearly removes a substantial amount of ^{210}Pb activity near the top of the coral. However, regardless of the nature of the cleaning, the base of all three transects returns to a constant value of about 0.3 dpm/g, although the bottom-most samples show a slight increase in all cases. ^{226}Ra is nearly constant in this coral, showing values close to the lowest activity of ^{210}Pb and indicating that little secondary ^{210}Pb has been added near the bottom of the coral in the last ~100 years (5+ half-lives).

4. Discussion

From the results above, it is clear that chemical cleaning of deep-sea corals before ^{210}Pb analysis is an important step to separate initial ^{210}Pb$_{ex}$ contained within the skeleton from ^{210}Pb added after the

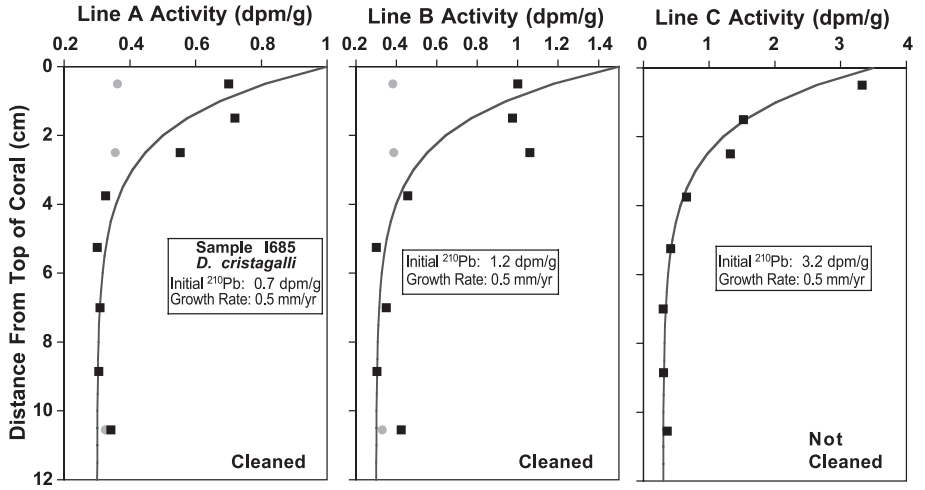

Fig. 4. ^{210}Pb (black squares) and ^{226}Ra (gray circles) data from *D. cristagalli* sample I685. Error bars are smaller than the symbol size. The three gray lines are model results using a constant growth rate of 0.5 mm/yr in each case. Models for the three transects differ in their initial ^{210}Pb activity. Subsamples in lines A and B were chemically cleaned, as described in the Methods section. Subsamples in line C were mechanically, but not chemically, cleaned.

skeleton has formed. This cleaning is not nearly as important for ^{226}Ra, which has a reasonably constant activity in both mechanically cleaned (G200, Fig. 1) and chemically cleaned (I685, Fig. 4) samples. These observations are consistent with the marine geochemistry of the two elements. While radium is soluble in seawater, lead is known to scavenge to surfaces [23,24] and has a short oceanic residence time.

The simplest explanation of the data is that ^{210}Pb resides in two forms in deep-sea corals—one bound in the aragonite skeleton and one added to its surface. However, it is possible that the ^{210}Pb added to the surface is contained in more than one phase, and that not all of these phases are removed by our chemical cleaning. For instance, lead might be moving from a more labile phase soon after deposition on the exterior to a more refractory environment as the coral ages. However, the cleaning study presented here can only distinguish total lead from nonleachable lead and so cannot resolve this issue. Nevertheless, it is clear that a leachable phase is being removed from the coral surface during chemical cleaning, and that subsamples near the bottoms of corals are always in secular equilibrium after the chemical treatment.

Eq. (1) describes model curves of activity versus distance from the growing coral tip that are dependent on two parameters, growth rate and initial ^{210}Pb activity ($^{210}Pb_{ex}^{0}$). With these two unknowns, a single $^{210}Pb_{ex}$ activity profile cannot uniquely determine a coral's growth rate. However, exponential decreases in $^{210}Pb_{ex}$ with distance from the coral tip are most readily explained by radioactive decay from a constant $^{210}Pb_{ex}^{0}$ value. To generate such an exponential profile through changing $^{210}Pb_{ex}^{0}$ would require a remarkable coincidence and is therefore unlikely. In addition, consistency of radionuclide concentrations between several transects within a single coral implies that all parts of the coral skeleton are responding to the same variables, including growth rate and the distribution coefficient for ^{210}Pb (D_{Pb}).

Although it was not chemically cleaned, *D. cristagalli* sample G200 shows a clear decrease in $^{210}Pb_{ex}$ from top to bottom that is consistent with closed-system first order decay (dark gray lines in Fig. 1). Apart from a small amount of secondary lead added to the bottom of transect A, each transect shows a consistent growth rate of about 2 mm/yr with the same $^{210}Pb_{ex}^{0}$. The extra ^{210}Pb observed at the bottom of transect A probably comes from colonizing organisms that recruited onto the lower parts of *D. cristagalli* sometime after the skeleton was formed.

Consistency between modeled growth rates is also seen for the three profiles of *D. cristagalli* sample I685, where, regardless of the cleaning protocol, each profile suggests a growth rate of 0.5 mm/yr. Deviations from first-order decay near the top of lines A and B could be due to limited variability in $^{210}Pb_{ex}^{0}$. The data from these two lines are also consistent with a step change in growth rate, or even a hiatus in growth, near the top of the coral. But the consistent modeled growth rate between three separate lines argues against this and suggests modest changes in $^{210}Pb_{ex}^{0}$ instead. Incomplete cleaning might also explain the deviations from simple decay, but all three profiles have consistent ^{210}Pb activities near the base, even with visual evidence for encrustation by other organisms (Fig. 3, spots in samples 5 and 6), indicating that cleaning was efficient. However, the more homogeneous bottom of I685 could also be due to the fact that this older portion has had more time to reach secular equilibrium and thus erase any initial variability in $^{210}Pb_{ex}^{0}$. Overall, the chemical cleaning method solves the problem of ^{210}Pb enrichments below a coral's growing edge (Figs. 1 and 2 as compared to Figs. 3 and 4). But our cleaning technique also reveals a level of variability in the upper portions of the *D. cristagalli* samples that we interpret as real variation in skeletal ^{210}Pb.

From these data, we cannot rule out the possibility of a variable D_{Pb}. By assuming that the ^{210}Pb activity of ~6 dpm/g observed at ~400 m at nearby GEOSECS Station #296 is similar to that seen at the location of growth of these three *D. cristagalli* samples and back correcting for the time of collection, our data support a range of distribution coefficients from 3 to 20 for the various samples. These results are higher than the value of 2.3 for D_{Pb} in surface corals from Bermuda [25], but, like D_{Ra}, they are similar to the maximum value of ~8 in a previously measured single Atlantic deep-sea coral [16]. For the two modeled *D. cristagalli* corals, there is an inverse relationship between $^{210}Pb_{ex}^{0}$ and the linear extension rate of the coral, perhaps implying that slower growth rates allow more time to scavange Pb from seawater.

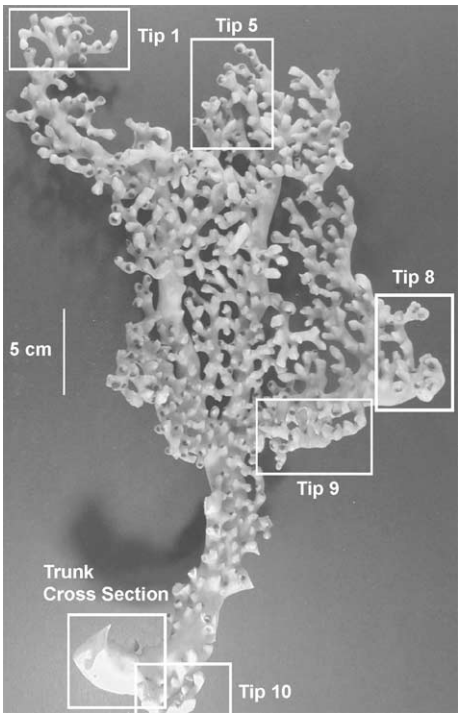

Fig. 5. Photograph of *E. rostrata* sample ALV 3701-8. Sample locations for the tips and the trunk cross-section are indicated by white boxes.

The constant growth rates regardless of cleaning status observed in coral I685 (Fig. 4) imply that much of the secondary ^{210}Pb is added at or near the time of skeletal growth. The additional ^{210}Pb activity at the top of this sample exceeds the ^{210}Pb trapped in the skeletal lattice by a factor of 3–5, but all sampled profiles still show a consistent growth rate of 0.5 mm/yr. One explanation for this observation is that secondary ^{210}Pb activity is elevated due to incorporation into the coral's organic tissue which then adheres to the coral skeleton and follows the growing edge of the skeleton. Although ^{210}Pb can occur both in the coral's aragonite lattice and on the exterior of the skeleton as a residual organic phase, each phase seems to follow the upward extension of the skeleton. As we have demonstrated in *D. cristagalli* sample S130 (Fig. 2), the organic tissue at the growing edge is

Table 2
^{210}Pb activities in the tips and base of *E. rostrata* sample ALV 3701-8

Sample	Distance from bottom (cm)	Pb-210 dpm/g	Error
Tip 1	46.8	0.195	0.003
Tip 5	41.5	0.164	0.002
Tip 8	34.4	0.159	0.003
Tip 9	32.4	0.188	0.005
Tip 10	9.0	0.108	0.004
Bottom of trunk		0.065	0.003

Errors are calculated from counting statistics. The range of activities in the tips implies that not all portions of this living sample grow at the same time or at the same rate.

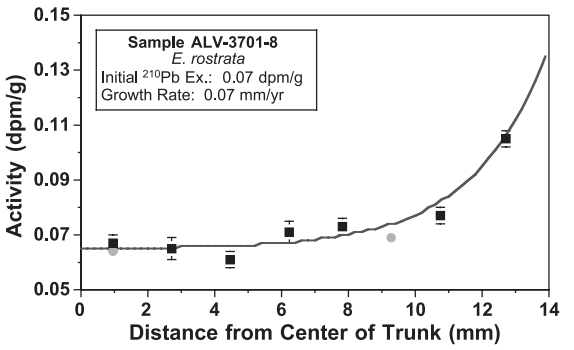

Fig. 6. ^{210}Pb (black squares) and ^{226}Ra (gray circles) data from the radial transect across the base of sample ALV 3701-8. The gray line is the model result for a constant growth rate of 0.07 mm/yr and a $^{210}Pb_{ex}^{0}$ of 0.07 dpm/g. The inner 8 mm of the trunk is consistent with secular equilibrium between ^{210}Pb and ^{226}Ra.

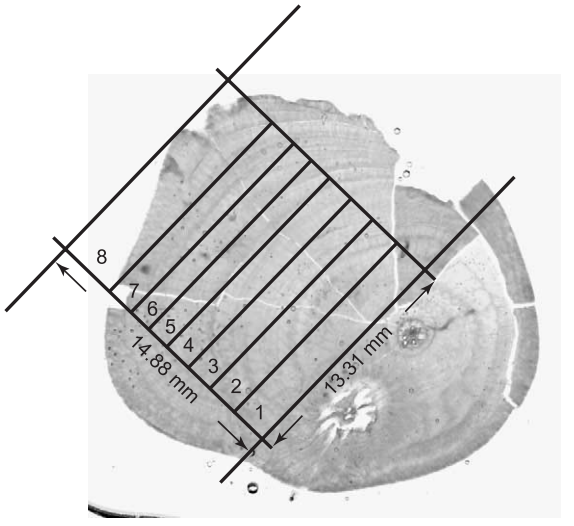

Fig. 7. Photograph of banding in the trunk of sample ALV 3701-8. Black lines show where individual samples were cut with a Dremel tool.

not the only source of nonlattice bound ^{210}Pb. The middle portion of that sample has the highest ^{210}Pb activity, but overall sample S130 seems to be near secular equilibrium and therefore much older than the other samples. A moving organic layer that does not "spill" very far over the *D. cristagalli* edge is consistent with the coral's growth history based on analyzing the skeleton's density bands [26,27].

We also measured transects of ^{210}Pb and ^{226}Ra activity in a second species of deep-sea scleractinian. A living *E. rostrata* (ALV 3701-8) was collected from the submersible Alvin at 1410-m depth on the North Bermuda slope in September 2001 (Fig. 5). ^{210}Pb activity in the tips of this sample was more variable than we expected (Table 2). The factor-of-two range in concentration implies that not all tips are growing at the same time, or that not all tips grow with the same D_{Pb}. While there was intact organic matter on tip 10, it either stopped incorporating ^{210}Pb sometime before we collected the sample, or it has a lower D_{Pb} than other parts of the coral. Assuming the center of the base is at secular equilibrium, the age difference between Tips 1 and 10 is about two half-lives of ^{210}Pb, or about 40 years.

A transect of ^{210}Pb across the base of this coral shows an excess at the outer edge but secular equilibrium values at the center (Fig. 6). About 6 mm from the edge, ^{210}Pb activities are within error of the two ^{226}Ra points. The first order decay model for this transect implies a radial growth rate of 0.07 mm/yr. These data also constrain the coral's age to be greater than 5–6 ^{210}Pb half-lives (about 100–130 years) and, if trunk thickening occurs at a uniform rate, suggest an age of ~210 years. As tip 1 is about 50

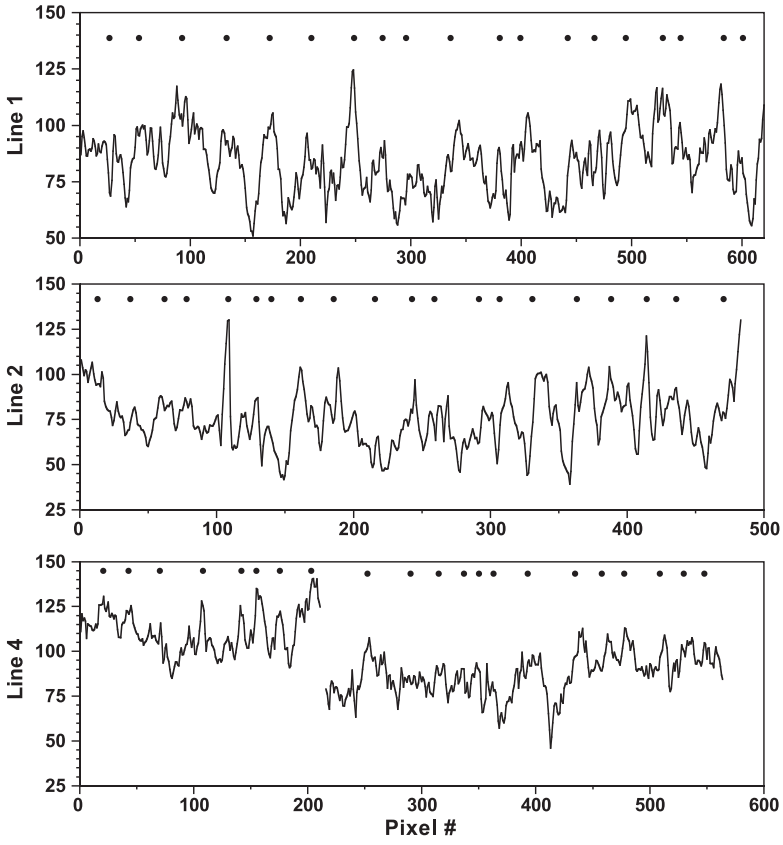

Fig. 8. Gray scale variation across three radial lines taken from the photograph in Fig. 7. Regular maxima in the gray scale are indicated by black dots. In each case, there are ~20 bands. Given the ^{210}Pb determined growth rate, these bands are not consistent with annual periodicity and occur, on average, every 10 years.

cm tall, we calculate a maximum vertical extension rate for this coral of ~5 mm/yr.

Using a 200-μm thick section of the base and a transmitted light photograph, we can image the radial growth bands in sample ALV 3701-8 (Fig. 7). With the free software NIH Image (http://rsb.info.nih.gov/nih-image/), we measured the radial gray scale variability in the region where we sampled for ^{210}Pb. Three separate transects across the coral's radius (Fig. 8) show consistent results of 19–21 growth bands. Given the 0.07 mm/yr radial growth rate calculated using the ^{210}Pb activities and the 15-mm radial distance, these gray scale data suggest only one band about every 10 years in *E. rostrata*. High-resolution climate records from this species cannot therefore rely on band counting of this type to constrain the chronology. However, with independent growth rate estimates (from ^{210}Pb for instance), both radial and particularly vertical sampling of single individuals will provide records covering over 100 years of ocean variability.

5. Conclusions

To isolate ^{210}Pb trapped in the aragonite lattice from that contaminating the surface, it is necessary to both mechanically and chemically clean deep-sea coral samples. ^{226}Ra activities on the other hand do not seem to be affected by the thoroughness of cleaning. We find a range of extension rates in *D. cristagalli* of 0.5–2.0 mm/yr with a reasonably constant value for each individual. A single *E. rostrata* sample grew faster with a vertical extension rate of ~5 mm/yr and a radial growth rate of ~0.07 mm/yr near its base. Based on this study and on historical data, different deep-sea scleractinia species have very different vertical extension rates. *D. cristagalli* is the slowest, while *Lophelia* sp. and *E. rostrata* extend faster. This difference means that *D. cristagalli* samples contain several decades or even more than 100 years of growth and are therefore good archives of decadal change in the deep ocean, providing resolution comparable to that of ice core records from the last glacial period. *E. rostrata* and *Lophelia* will provide higher resolution and perhaps even annual records. Growth morphologies in *D. cristagalli* and *E. rostrata* make these two species especially well suited to paleoceanographic studies.

Acknowledgements

We thank Will Berelson and T.L. Ku at USC for their help with the ^{209}Po spike. Marty Fleisher at LDEO alpha counted our silver disks and helped interpret the energy spectra. JFA and JSLW were supported by NSF grant OCE-0096373. We also thank the WHOI Alvin group and the crew of the Atlantis for recovering sample ALV 3701-8.

Appendix A. Supplementary data

Supplementary data associated with this article can be found in the online version at doi:10.1016/j.epsl.2004.08.022.

References

[1] J.E. Cole, R.G. Fairbanks, G.T. Shen, Recent variability in the Southern Oscillation: isotopic records from a Tarawa Atoll coral, Science 260 (1993) 1790–1793.
[2] A.W. Tudhope, C.P. Chilcott, M.T. McCulloch, E.R. Cook, J. Chappell, R.M. Ellam, D.W. Lea, J.M. Lough, G.B. Shimmield, Variability in the El Nino-Southern oscillation through a glacial–interglacial cycle, Science 291 (2001) 1511–1517.
[3] K. Cobb, C. Charles, H. Cheng, R.L. Edwards, El Nino/Southern oscillation and tropical Pacific climate during the last millennium, Nature 424 (2003) 271–276.
[4] K.A. Hughen, D.P. Schrag, S.B. Jacobsen, W. Hantoro, El Nino during the last interglacial period recorded by a fossil coral from Indonesia, Geophysical Research Letters 26 (1999) 3129–3132.
[5] R.G. Fairbanks, R.E. Dodge, Annual periodicity of the ^{18}O/^{16}O and ^{13}C/^{12}C ratios in the coral *Montastrea annularis*, Geochimica et Cosmochimica Acta 43 (1979) 1009–1020.
[6] S.W. Knutson, R.W. Buddemeier, S. Smith, Coral chronometers: seasonal growth bands in reef corals, Science 177 (1972) 270–272.
[7] W.S. Moore, S. Krishnaswami, Coral growth rates using Ra-228 and Pb-210, Earth and Planetary Science Letters 15 (1972) 187–190.
[8] W.S. Moore, S. Krishnaswami, S.G. Bhat, Radiometric determinations of coral growth rates, Bulletin of Marine Science 23 (1973) 157–176.
[9] R.E. Dodge, J. Thomson, The natural radiochemical and growth records in contemporary hermatypic corals from the Atlantic and Caribbean, Earth and Planetary Science Letters 23 (1974) 313–322.
[10] J.E. Smith, H.P. Schwarcz, M.J. Risk, T.A. McConnaughey, N. Keller, Paleotemperatures from deep-sea corals: overcoming 'vital effects', Palios 15 (2000) 25–32.

[11] A. Mangini, M. Lomitschka, R. Eichstadter, N. Frank, S. Vogler, G. Bonani, I. Hajdas, J. Patzold, Coral provides way to age deep water, Nature 392 (1998) 347–348.
[12] J.F. Adkins, H. Cheng, E.A. Boyle, E.R.M. Druffel, L. Edwards, Deep-sea coral evidence for rapid change in ventilation of the deep North Atlantic 15,400 years ago, Science 280 (1998) 725–728.
[13] P.M. Duncan, On the rapidity of growth and variability of some Madreporaria on an Atlantic cable with remarks upon the rate of accumulation of foraminiferal deposits, Annals & Magazine of Natural History 20 (1877) 361–365.
[14] J.B. Wilson, Patch development of the deep-water coral *Lophelia pertusa* (L.) on Rockall bank, Journal of the Marine Biology Association 59 (1979) 165–177.
[15] N. Bell, J. Smith, Coral growing on North Sea oil rigs, Nature 402 (1999) 601.
[16] E.R.M. Druffel, L.L. King, R.A. Belastock, K.O. Buesseller, Growth rate of a deep-sea coral using ^{210}Pb and other isotopes, Geochimica et Cosmochimica Acta 54 (1990) 1493–1500.
[17] M.J. Risk, J.M. Heikoop, M.G. Snow, R. Beukens, Life spans and growth patterns of two deep-sea corals: *Primnoa resedaeformis* and *Desmophyllum cristagalli*, Hydrobiologia 471 (2002) 125–131.
[18] J.F. Adkins, S. Griffin, M. Kashgarian, H. Cheng, E.R.M. Druffel, E.A. Boyle, R.L. Edwards, C.-C. Shen, Radiocarbon dating of deep-sea corals, Radiocarbon 44 (2002) 567–580.
[19] H. Cheng, J.F. Adkins, R.L. Edwards, E.A. Boyle, U–Th dating of deep-sea corals, Geochemica et Cosmochemica Acta 64 (2000) 2401–2416.
[20] J.F. Adkins, E.A. Boyle, Age screening of deep-sea corals and the record of deep North Atlantic circulation change at 15.4 ka, in: F. Abrantes, A. Mix (Eds.), Reconstructing Ocean History: A Window into the Future, Kluwer, New York, 1999.
[21] W.W. Flynn, The determination of low levels of polonium-210 in environmental samples, Analytica Chimica Acta 43 (1968) 221–227.
[22] D.A. Foster, M. Staubwasser, G.M. Henderson, ^{226}Ra and Ba concentrations in the Ross Sea measured with multi-collector ICP mass spectrometry, Marine Chemistry 87 (2004) 59–71.
[23] M.P. Bacon, D.W. Spencer, P.G. Brewer, Pb-210/Ra-226 and Po-210/Pb-210 disequilibria in seawater and suspended particulate matter, Earth Planet. Sci. Lett. 32 (1976) 277–296.
[24] M.P. Bacon, D.W. Spencer, P.G. Brewer, Lead-210 and polonium-210 as marine geochemical tracers: review and discussion of results from the Labrador Sea, in: T.F.G.a.W.F. Lowder (Ed.), Natural Radiation in the Environment II, 1978, pp. 473–501 USDA CONF-780422.
[25] G.T. Shen, E.A. Boyle, Lead in corals: reconstruction of historical industrial fluxes to the surface ocean, Earth Planet Science Letters 82 (1987) 289–304.
[26] J.E. Sorauf, J.S. Jell, Sturcture and incremetal growth in the ahermatyic coral *Desmophyllum cristagalli* from the North Atlantic, Paleontology 20 (1977) 1–19.
[27] A.V. Lazier, J.E. Smith, M.J. Risk, H.P. Schwarcz, The skeletal structure of *Desmophyllum cristagalli*: the use of deep-water corals in sclerochronology, Lethaia 32 (1999) 119–130.